Journal of Hazardous Materials 476 (2024) 134935

Contents lists available at ScienceDirect

Journal of Hazardous Materials

journal homepage: www.elsevier.com/locate/jhazmat

Research Paper

Novel cross-linkable fluorescent probe with oriented antibody to enhance lateral immunoassay strip for the detection of acetamiprid

Donghan Li [a,b,c], Haowei Dong [a,b,c], Zhengtao Li [a,b,c], Haifang Wang [d], Jiashuai Sun [a,b,c], Jingcheng Huang [a,b,c], Peisen Li [a,b,c], Shuxian Zhou [a,b,c], Shengxi Zhai [a,b,c], Mingxin Zhao [e], Xia Sun [a,b,c,*], Yemin Guo [a,b,c,*]

[a] School of Agricultural Engineering and Food Science, Shandong University of Technology, No. 266 Xincun Xilu, Zibo, Shandong 255049, China
[b] Shandong Provincial Engineering Research Center of Vegetable Safety and Quality Traceability, No. 266 Xincun Xilu, Zibo, Shandong 255049, China
[c] Zibo City Key Laboratory of Agricultural Product Safety Traceability, No. 266 Xincun Xilu, Zibo, Shandong 255049, China
[d] Dongzhimen Hospital, Beijing University of Chinese Medicine, Beijing 100700, China
[e] Institute of Fruit and Floriculture of Gansu Academy of Agricultural Sciences, Lanzhou, Gansu 730070, China

HIGHLIGHTS

- TRFLIS offers rapid, reliable detection of acetamiprid.
- Introducing GaMIgG as sandwich protein for enhancing probe sensitivity.
- Innovative use of cross-linking agent enhances probe stability.
- This strategy prominent reduced antibody dosage.
- A low-cost, high-performance immunochromatographic platform was constructed.

GRAPHICAL ABSTRACT

Fig. 1. Synthesis of TRFM-GaMIgG-AAb and the principle of TRFLIS for acetamiprid detection.

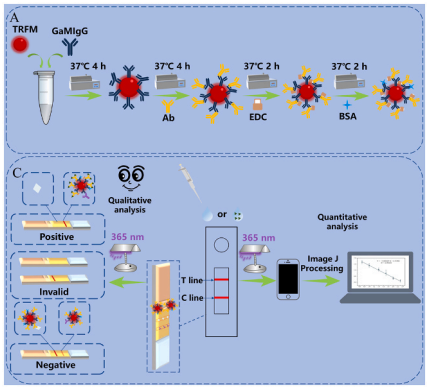

ARTICLE INFO

Keywords:
Time-resolved fluorescent microsphere
Goat anti-mouse IgG
Vegetables
Immunochromatographic platform
1-ethyl-(3-dimethylaminopropyl) carbodiimide hydrochloride

ABSTRACT

Time-resolved fluorescent lateral immunoassay strip (TRFLIS) is a reliable and rapid method for detecting acetamiprid. However, its sensitivity is often affected by the structural patterns and stability of the fluorescent probe. Researchers have shown significant interests in using goat anti-mouse IgG (GaMIgG) which is indirectly bound to time-resolved fluorescent microsphere (TRFM) and antibody. This allowed for oriented modification of the antibody. However, the stability of fluorescent probe in this binding mode remained unexplored. Herein, 1-ethyl-(3-dimethylaminopropyl) carbodiimide hydrochloride was innovatively used as a cross-linking agent to enhance the binding of antibody to GaMIgG, which improved the stability of the fluorescent probe. Under optimal working conditions, this strategy exhibited a wide linear response range of 5–700 ng/mL. Its limit of

* Corresponding authors at: School of Agricultural Engineering and Food Science, Shandong University of Technology, No. 266 Xincun Xilu, Zibo, Shandong 255049, China.
E-mail addresses: sunxia2151@sina.com (X. Sun), gym@sdut.edu.cn (Y. Guo).

https://doi.org/10.1016/j.jhazmat.2024.134935
Received 21 March 2024; Received in revised form 12 June 2024; Accepted 14 June 2024
Available online 15 June 2024
0304-3894/© 2024 Published by Elsevier B.V.

detection (LOD) was 0.62 ng/mL, the visual LOD was 5 ng/mL, and the limit of quantification (LOQ) of 2.06 ng/mL. Additionally, under tomato matrix, leek matrix and Chinese cabbage matrix, the linear response ranges were 5–400, 5–300, and 5–700 ng/mL, with LODs of 0.16, 0.60, and 0.41 ng/mL, with LOQs of 0.53, 2.01 and 1.37 ng/mL, respectively. In conclusion, this strategy effectively reduced the dosage of acetamiprid antibody compared with TRFM directly linking acetamiprid antibody, and greatly increased the sensitivity of TRFLIS. Meanwhile, it demonstrated outstanding specificity and accuracy in acetamiprid detection and had been successfully applied to vegetable samples. This method enables rapid and accurate detection of large-volume samples by combining qualitative and quantitative methods. As such, it has great potential in the development of low-cost and high-performance immunochromatographic platforms.

1. Introduction

Acetamiprid (ACE) is a neonicotinoid insecticide known for its high efficiency and broad-spectrum effectiveness in agriculture. It is extensively used to control various pests, such as false-eye leafhoppers, thrips, and aphids [23]. While ACE is beneficial in pest management, the issue of pesticide residues on vegetables has been receiving significant attention. Short-term exposure to ACE has the potential to disrupt the endocrine system [3], while long-term exposure may increase the risk of cancer and pose detrimental effects on reproductive health [34].

Due to the trace amounts of ACE residues in vegetables, detection methods must have high sensitivity, precision, stability, and exceptional specificity. Classical analytical methods for the determination of ACE in vegetables were mainly liquid chromatography [44], liquid chromatograph-mass spectrometer [13], and so on. However, these sophisticated methods were not suitable for detecting large quantity of samples in real time administration. For decades, a variety of novel analytical methods have been developed tremendously and used for the determination of ACE, including enzyme-linked immunosorbent assay (ELISA) [7], electrochemiluminescence (ECL) [36], surface-enhanced Raman spectroscopy (SERS) [6], colorimetry [39] and so on. However, the shortcomings of these methods include the relatively high instrument cost, complexity of the procedures, relatively long analysis times. Therefore, these methods are not suitable for on-site examination of food safety. In contrast, lateral immunoassay strip has simple operations, fast detection speeds, and maintain high detection accuracy over a wide range of temperatures and humidities.

Time-resolved fluorescent lateral immunoassay strip (TRFLIS) has attracted considerable interests among researchers as a simple and cost-effective on-site detection method [33]. Li et al. developed a ceftiofur fluorescent probe by coupling a specific antibody directly to time-resolved fluorescent microsphere (TRFM), and the limit of detection of ceftiofur was 0.97 ng/mL [20]. The signal probe was created by combining TRFM with the target antibody, and it bound specific targets on nitrocellulose (NC) membranes via lateral chromatography reaction [38]. Under this strategy, antibody bound to TRFM is stochastic, which leads to the potential for antigenic determinant on antigen-binding fragment to be covered or spatial site resistance to be affected, resulting in a reduced ability to bind antigens [8].

To increase the binding efficiency of the target antibody to the TRFM, a sandwich protein is often introduced. This indirect coupling mechanism [15,26,42] results in significantly enhanced fluorescence signal intensity of the detection system compared with the target antibody directly coupled to TRFM. Protein A [21], protein G [30] and secondary antibody [43] are commonly used as sandwich proteins, targeting the fragment crystallized (Fc) region directly with bio affinity. Chakraborty et al. [2] and Li et al. [22] significantly improved the sensitivity of the sensors by introducing protein G and protein A respectively. Furthermore, research had demonstrated that the resulting target antibody had the best binding effect on the antigen when the secondary antibody was oriented to modify the target antibody [14,16]. Li et al. [18], Dong et al. [5], and Sun et al. [35] used a secondary antibody as a sandwich protein to immobilize the target antibody to form a fluorescent probe. This strategy improved the sensitivity of the test strips and reduced the dosage of antibody. However, this strategy that introduced the secondary antibody did not undergo centrifugation following the coupling process with the target antibody. This resulted in that the unbinding target antibody was not being separated from the probe, potentially impacting the sensitivity of the TRFLIS. The lack of centrifugation might be the disruption of binding between the secondary antibody and the target antibody by the mechanical stress of centrifugation [24]. 1-ethyl-(3-dimethylaminopropyl) carbodiimide hydrochloride (EDC) was a crosslinking agent used in material synthesis to improve bonding strength [9]. Masoud Salavati's team used EDC as a cross-linker during the hydrogel synthesis process to improve the mechanical strength and stability of the hydrogels [10]. In the field of biomolecules EDC was also used as a cross-linking agent to improve binding strength [12]. Nair et al. [32] employed EDC to enhance the binding strength between collagens. Bax et al. [1] utilized EDC to crosslink collagen with elastin. Lou et al. [24] utilized EDC as a cross-linking agent to enhance the binding strength between protein G and antibody, and they compared the amount of antibody immobilized by four distinct synthesis methods. Although some immunosensors utilizing EDC as a cross-linking agent had been developed, it should be noted that there was nearly no report about EDC as a crosslinking agent for probe synthesis of sandwich protein with secondary antibodies. High sensitivity could be expected if such a novel method was used for probe synthesis.

Herein, a novel cross-linkable fluorescent probe with oriented antibody was constructed. The probe utilized goat anti-mouse IgG (GaMIgG) as a sandwich protein and acetamiprid antibody (AAb) as a sensitive recognition element. Meanwhile, the formation of covalent bonded between GaMIgG and AAb in the TRFM-GaMIgG-AAb complex was facilitated by the utilization of EDC as a cross-linking agent, thereby increasing the bonding strength. The optimal preparation process and working conditions of TRFLIS were optimized and the working curve of TRFLIS was obtained. The detection performance of TRFLIS was also evaluated and the TRFLIS was used for testing vegetable samples. Thus, the proposed TRFLIS based strategy of a novel cross-linkable fluorescent probe with oriented antibody holds a great application potential for improving the existing detection of acetamidine. And this strategy has a wide range of market application potential, especially suitable for meeting the needs of rapid daily testing.

2. Materials and methods

2.1. Chemical reagents and materials

N-hydroxysuccinimide (NHS) and EDC were procured from Shanghai McLean Biochemical Technology Co., Ltd. Triton X-100 and acetamiprid standards were obtained from Aladdin Biochemical Technology Co., Ltd. PVP-K30 was supplied by Tianjin Bodi Chemical Co., Ltd. Bovine serum albumin (BSA) was procured from USA Sigma-Aldrich. The complex solution, coating solution, backing plates, absorbent pads, sample pads, conjugate pads, NC membranes, and TRFM (concentration: 1 mg/mL, grain diameter 300 nm, excitation wavelength: 365 nm, emission wavelength: 610 nm, color: red fluorescence) were procured from Shandong Landu Biotechnology Co., Ltd. The AAb, acetamiprid antigen

(ACE-BSA), GaMIgG, and rabbit anti-goat IgG (RaGIgG) were procured from Beijing Biodragon Immunotechnologies Co., Ltd. Methanol, sucrose, KCl, NaCl, Na_2HPO_4, and KH_2PO_4 were procured from Shanghai Sinopharm Chemical Reagent Co., Ltd.

2.2. Instruments

Fluorescence spectrophotometer (RF-6000) from Japan Shimadzu. The microcomputer automatic chopper (ZQ3500), and the XYZ 3D film

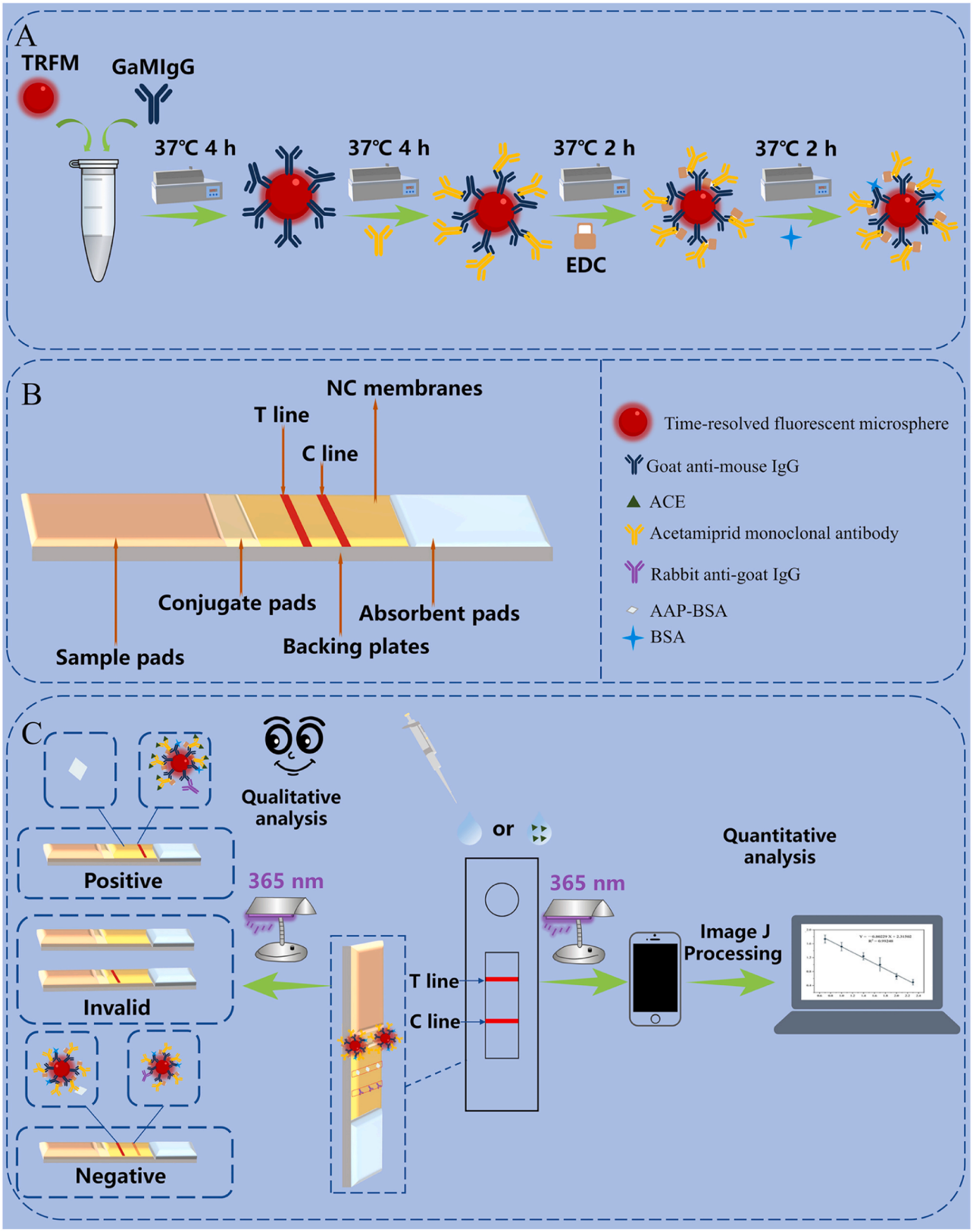

Fig. 1. Synthesis of TRFM-GaMIgG-AAb(A); Assembly of TRFLIS (B); Diagram illustrating the principle of TRFLIS for acetamiprid detection(C).

sprayer (HM3035) from Shanghai Gold Standard Biotechnology Co., Ltd. The transmission electron microscope (Tecnai G2 20) from USA Thermo Fisher Scientific. The vortex mixer (KV37-Vortex Genie 2) from the USA Scientific Industries. High sensitivity zeta potential analyzer (Nanobrook 90Plus Zeta) from USA Brookhaven Instruments Co., Ltd. Precision electronic balance (AL104) from Mettler-Toledo. In addition, the constant temperature oscillating water bath (SHA-C) from Zhengzhou Honghua Instrument Co., Ltd. High-temperature blast dryer (DHG-9240A) from Shanghai Yiheng Technology Co., Ltd. Triple UV analyzer (ZF-1) from Haimen Kirin Bell Laboratory Instrument Co., Ltd. Smartphone (Huawei Mate 40) from Huawei Technologies Co., Ltd.

2.3. Synthesis of TRFM-GaMIgG-AAb

The 100 μL TRFM (1 mg/mL) was washed twice by PBS (0.072 g KH_2PO_4, 0.06 g KCl, 2.7 g NaCl, 1.086 g Na_2HPO_4 were dissolved in 1000 mL ultrapure water, pH 7.0, 0.006 M). After the addition of 20 μL NHS (20 mg NHS was dissolved in 1 mL 0.006 M PBS, 20 mg/mL), the mixture was incubated with oscillation for 2 min. And then, the 5 μL EDC (20 mg EDC was dissolved in 1 mL 0.006 M PBS, 20 mg/mL) and the TRFM were incubated oscillatively at 37 °C for 1 h to activate the carboxyl groups of the TRFM. The TRFM was washed by centrifugation (13,000 rpm, 12 min). The 4 μL GaMIgG (5 mg/mL) was added to the activated TRFM. Next, they incubated oscillatively at 37 °C for 4 h. The incubated solution was washed by centrifugation (13,000 rpm, 12 min) and resuspended to obtain the TRFM-GaMIgG. The TRFM-GaMIgG-AAb was obtained by adding 2 μL AAb (2 mg/mL) to the TRFM-GaMIgG. The solution was incubated oscillatively for 4 h at 37 °C. The addition of 2 μL EDC (10 mg EDC was dissolved in 1 mL 0.006 M PBS, 10 mg/mL), and the mixed solution was incubated with oscillation at 37 °C for 2 h. The purpose was to promote the binding of GaMIgG to AAb and thus increase the stability of TRFM-GaMIgG-AAb. After adding 100 μL of BSA (20 mg BSA was dissolved in 1 mL 0.006 M PBS, 20 mg/mL), the mixture was incubated with oscillation at 37 °C for 2 h. The solution was subjected to a final centrifugal washing (13,000 rpm, 12 min) and resuspension using complex solution (0.5 g BSA, 0.1 g polyethylene glycol 400, 0.025 g casein, 0.05 g lysine and 0.005 g HgS were dissolved in 100 mL 0.002 M PBS, pH 7.0). The TRFM-GaMIgG-AAb was finally obtained and stored at 4 °C. The preparation process is shown in Fig. 1A.

2.4. Test strips assembly and operation

Before assembly, the conjugate pads were immersed in a sealing buffer (0.4 g Triton X-100, 2 g sucrose, 0.5 g BSA were dissolved in 100 mL 0.002 M PBS, pH 7.0) and then dried at 37 °C for 1 h. The 0.1 mg/mL of TRFM-GaMIgG-AAb was evenly sprayed on the conjugate pads. Then, the conjugate pad was allowed to dry at 37 °C for 2 h. After being sprayed onto the conjugate pads, the TRFM-GaMIgG-AAb mixture was dried at 37 °C for 2 h. The ACE-BSA and RaGIgG were prepared by diluting them with the coating solution (0.4 g Triton X-100 was dissolved in 100 mL 0.002 M PBS, pH 7.0). Using XYZ 3D film sprayer (HM3035), ACE-BSA (0.02 mg/mL) and RaGIgG (0.1 mg/mL) were sprayed onto the test line (T line) and control line (C line) of the NC membranes at rate of 0.8 μL/cm. To assemble the test strips, first overlap the absorbent pads and conjugate pads with the NC membranes by approximately 1 mm. Then, overlap the sample pads with the conjugate pads by about 1 mm. According to the width of 3.8 mm/strip chopping, to obtain the TRFLIS. The specific positioning was illustrated in Fig. 1B.

The 80 μL sample solution was added dropwise onto a sample pad and it was incubated at 37 °C for 15 min. During the chromatographic process, ACE-BSA immobilized at the T line could specifically recognize AAb in TRFM-GaMIgG-AAb, while RaGIgG immobilized at the C line could specifically recognize GaMIgG in TRFM-GaMIgG-AAb. Under the competition principle illustrated in Fig. 1C, the absence of ACE in the sample led to TRFM-GaMIgG-AAb binding to ACE-BSA in the T line through the absorbent pad's action, resulting in a red fluorescent band in the T line. Simultaneously, the fluorescence signal at the C line was weakened as most of the TRFM-GaMIgG-AAb was captured by the T line. Conversely, in the presence of ACE, it bound to the antigen binding site of TRFM-GaMIgG-AAb, which caused RaGIgG to capture GaMIgG on TRFM-GaMIgG-AAb, weakened the fluorescence signal in the T line and enhanced it in the C line. Moreover, the absence of color in the C line indicated the invalidity of the TRFLIS. These results could be observed qualitatively with a naked eye and quantitatively using Image J.

2.5. Sample pre-treatment

The leek, Chinese cabbage, and tomato samples were homogenized by being allocated into a 50 mL centrifuge tube with 5 g of the sample and then supplemented with 10 mL of methanol. Following this, the concoction underwent ultrasonication for 15 min and was subsequently centrifuged at 3000 rpm for 15 min. Finally, the supernatant was passed through a 0.22 μm organic filter film to eliminate impurities.

2.6. Data analysis

The TRFLIS was placed onto a 365 nm UV analyzer, and photos were taken using a Huawei Mate 40 smartphone. The obtained images were imported into ImageJ software and transformed into 8-bit grayscale representations. Subsequently, the grayscale values of the strip were obtained by framing the strip using a rectangle tool. The study gained the gray scale values of the T line (T) and C line (C) in positive samples, as well as the grayscale values of the T (T_0) and C (C_0) lines in negative samples using Image J. In addition, this study employed two ways to optimize the experimental parameters. Firstly, the study focused on the grayscale values of the T_0 and C_0, which represented the strength of the fluorescence signal in the absence of ACE. Secondly, the study assessed the rangeability of the T_0/C_0 in a negative sample and the T/C in positive sample. A higher rangeability represented a more desirable rate of change.

3. Results and discussion

3.1. Characterization of the TRFM-GaMIgG-AAb

To verify that the TRFM-GaMIgG-AAb was prepared successfully, transmission electron microscope (TEM), hydrodynamic diameter, and fluorescence spectral scans of the fluorescent probe were analyzed. Fig. 1A showed the TRFM constituted uniformly distributed spherical particles, uniform overall dispersion, and smooth ball edges. Fig. 2B showed the TRFM-GaMIgG and Fig. 2C showed the TRFM-GaMIgG-AAb, respectively. They were irregular shape and irregular protrusions at the edges compared with Fig. 2A. Moreover, because AAb could be attached to multiple GaMIgG, TRFM-GaMIgG-AAb resulted in further aggregation of TRFM compared with TRFM-GaMIgG. Therefore, the successful preparation of the TRFM-GaMIgG-AAb could be inferred from the TEM. Dynamic light scattering analysis showed that the TRFM, TRFM-GaMIgG and TRFM-GaMIgG-AAb had average hydrodynamic diameters of 359 nm, 387 nm, 392 nm respectively (Fig. 2D). Therefore, the successful preparation of the TRFM-GaMIgG-AAb could be inferred from the change in particle size. Moreover, to confirm the success of the TRFM-GaMIgG-AAb preparation, spectral scans of the fluorescent were conducted both before and after the coupling process (Fig. 2E). It was observed that the peaks of TRFM coupled with GaMIgG and AAb exhibited a slight decrease compared with their before coupling. This decline could be attributed to the formation of a complex after TRFM sequential coupling with GaMIgG and AAb, resulting in partial quenching of the fluorescence signal and subsequent weakening of the overall fluorescence signal [4]. The diminished fluorescence signal signified the successful preparation of TRFM-GaMIgG-AAb. In addition, the impact of the cross-linker EDC on the fluorescence signal was explored in the study. Analyzed from Fig. 2D revealed that the addition

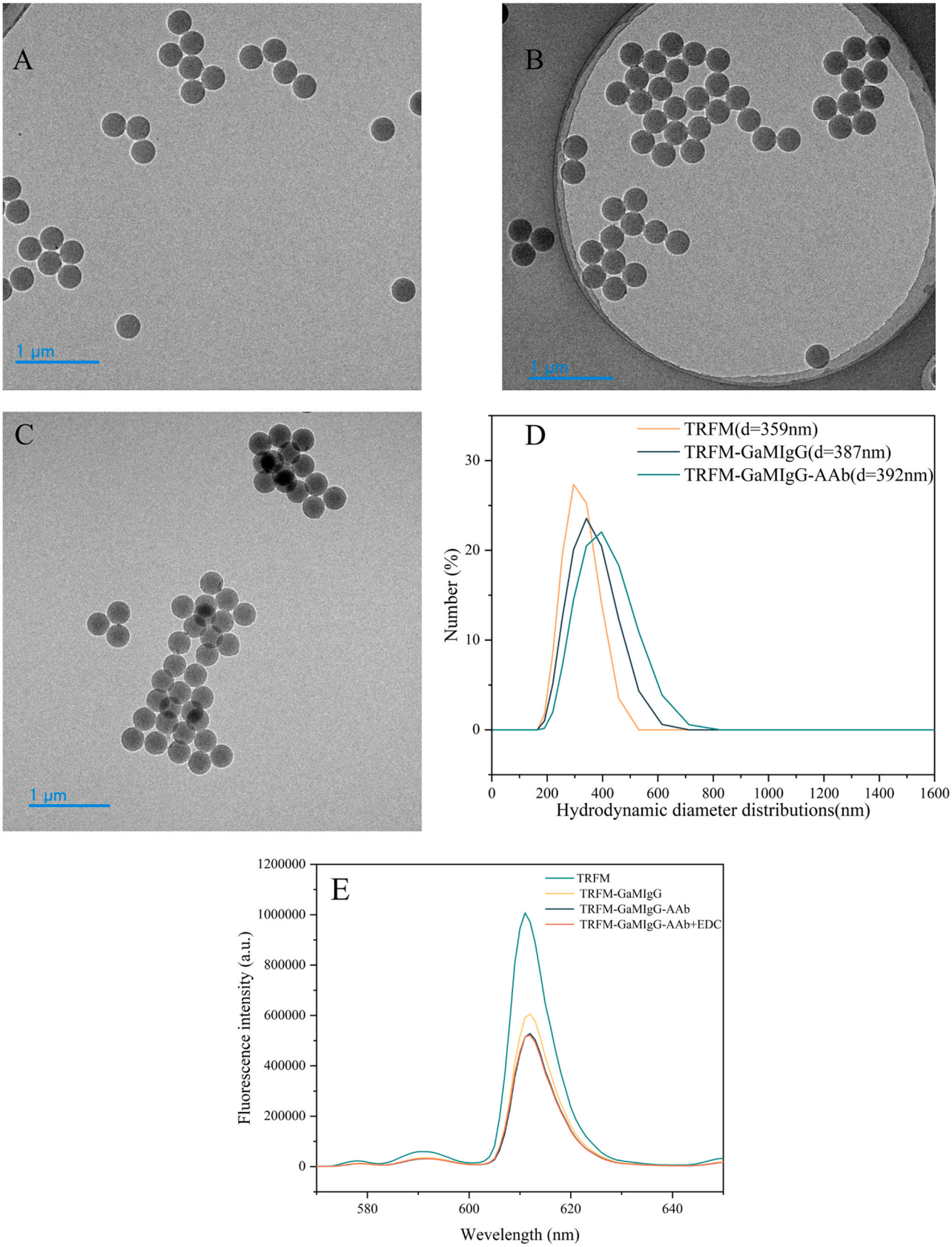

Fig. 2. TEM image of TRFM (A), TRFM-GaMIgG (B) and TRFM-GaMIgG-AAb (C); Hydrodynamic diameter distributions of TRFM, TRFM-GaMIgG, TRFM-GaMIgG-AAb and TRFM-GaMIgG-AAb+EDC (D); Fluorescence spectra of TRFM, TRFM-GaMIgG, TRFM-GaMIgG-AAb and TRFM-GaMIgG-AAb+EDC (E).

of EDC did not affect the fluorescence signal.

3.2. Optimization of TRFLIS parameters

A suitable concentration of the PBS facilitated sufficient binding of the target molecules bound to the TRFM [17]. Therefore, the concentrations of PBS (0.002, 0.004, 0.006, 0.01 and 0.02 M) were optimized. The bar graph in Fig. 3A depicted the T_0 and C_0, which exhibited a gradual increase with higher PBS concentrations. Specifically, T_0 and C_0 peaked at 0.006 M PBS concentration. Analyzing the line graph, it showed the T_0/C_0 and T/C rangeability at each PBS concentration, with a larger rangeability indicating a superior rate of change. Notably, when the concentration of PBS was 0.006 M, the TRFLIS could obtain a better rate of change. Consequently, the optimal concentration of PBS was 0.006 M.

TRFM might lose its stability under acidic or alkaline conditions, leading to a decrease in binding efficiency [19]. Furthermore, different pH might affect the binding efficiency between GaMIgG and TRFM as well as AAb. Hence, the pH of PBS (5, 6, 7, 8 and 9) was optimized to improve the sensitivity of TRFLIS. The experimental resulted in Fig. 3B showed that T_0 and C_0 exhibited an initial increase followed by a decreased with rising pH levels of the PBS, with a peak observed at pH 7. In addition, TRFLIS showed a better rate of change at pH 7, as the activity of the antibody was impaired at different pH. Therefore, it could be concluded that the TRFLIS exhibited optimal performance at pH 7.

In the coupling process, the GaMIgG served as a critical bridge between AAb and TRFM. Insufficient GaMIgG dosage hindered the effective coupling of TRFM. Conversely, an excessive amount of GaMIgG caused the aggregation of excessive protein material on the TRFM surface, leading to a decrease in fluorescent signals [5]. To investigate the optimal amount of GaMIgG, different dosages of GaMIgG (10, 20, 30, 40, and 50 μg) were added in the study. Fig. 3C showed that both T_0 and C_0 increased as the dosage of GaMIgG increased. It was observed that T_0 and C_0 reached their maximum values at the dosage of GaMIgG was 40 μg, suggesting that this dosage reached the coupling dosage. In addition, the rate of change at 40 μg was relatively lower compared with 20 μg and 30 μg. Consequently, considering cost-effectiveness and the overall performance of the TRFLIS, the TRFLIS performed best when the dosage of GaMIgG was 20 μg.

The used dosage of AAb determined the cost of TRFLIS. Minimizing AAb consumption while maintaining assay efficiency was a primary goal of antibody optimization. Higher AAb dosage could lead to reduce competition between ACE-BSA and ACE for AAb, thereby diminishing the sensitivity of the TRFLIS. Therefore, optimizing the AAb concentration not only enhanced the TRFLIS sensitivity but also contributed to cost savings. The probe was prepared by adding different dosages (2, 4, 8, 10, 12, and 16 μg) of AAb. The maximum values of T_0 and C_0 were observed at an AAb dosage of 8 μg, which might be due to the binding of 8 μg of AAb to GaMIgG reaching the saturation level from Fig. 3D. In addition, the rate of change showed a tendency to increase and then decrease as the dosage of AAb increased, with the most rate of change observed at 4 μg of AAb. Hence, the 4 μg was chosen as the optimal dosage of AAb from the perspective of saving the consumption of AAb.

Utilizing GaMIgG as a sandwich protein to form TRFM-GaMIgG-AAb could enhance the sensitivity of TRFLIS compared with traditional methods. However, vigorous centrifugal washing or prolonged storage under mild conditions might lead to AAb detached from TRFM-GaMIgG-AAb. The cross-linking agent EDC facilitated the formation of covalent bonds between GaMIgG and AAb, enhancing the binding strength of the TRFM-GaMIgG-AAb. To investigate the effect of EDC as a cross-linking agent, TRFM-GaMIgG-AAb were centrifuged and washed (1, 2, 4, and 6 times), with and without EDC. Subsequently, the fluorescence signals of the T and C lines were analyzed to assess the detachment of AAb. Fig. 3E illustrated that the fluorescence signals of the T and C lines remained relatively constant in the TRFLIS with EDC, suggesting effective binding of GaMIgG to AAb facilitated by EDC. On the contrary, without EDC, TRFLIS showed weakened fluorescence signals in the T line and enhanced fluorescence signals in the C line after multiple centrifugations. This observation might result from a reduction in the amount of TRFM-GaMIgG-AAb captured by the T line's ACE-BSA, likely caused by the detachment of AAb from TRFM-GaMIgG-AAb, subsequently increasing the capture by the C line's RaMIgG. Thus, it showed that the cross-linker EDC could form a covalent bond between GaMIgG and AAb, which improved the stability of the TRFM-GaMIgG-AAb.

EDC increased the binding strength of TRFM-GaMIgG-AAb, which increased the binding of AAb and ACE-BSA. Therefore, the optimal volume of EDC could be determined based on T_0. In Fig. 3F, it exhibited the maximum T_0 at the EDC volume of 2 μL, with T_0 decreased gradually as the volume of EDC increased. This phenomenon might be attributed to the use of lower levels of EDC, which effectively avoided negative effects from excessive cross-linking [24].

Methanol was often used as an organic solvent for ACE extraction from the sample. A low concentration of methanol in the matrix solution might result in inadequate extraction efficiency. Conversely, an excess of methanol might hinder the specific biological activities and sensitivities of AAb. The study evaluated the tolerance of TRFM-GaMIgG-AAb to methanol concentration and the results were shown in Fig. 3G. The fluorescence signals of the C and T lines of the TRFLIS remained normal within the range of methanol concentration from 0 % to 30 %. However, when the methanol concentration reached 40 % and above, the color development of the C and T lines was significantly weakened or even lost, suggesting a significant inhibition of TRFM-GaMIgG-AAb activity. In addition, the rate of change at methanol concentration with a normal degree of color development was also explored (the concentration of samples was 200 ng/mL). Fig. 3H illustrated that TRFLIS exhibited highest rate of change at a methanol concentration of 10 %.

3.3. Assessment of the TRFLIS

3.3.1. Sensitivity

To assess the functionality of the TRFLIS under optimal conditions, specified concentrations were detected using the instrument. The relationship between the logarithm of the concentration of ACE (X) and the ratio of T/C (Y) was studied. The fluorescence signals of TRFLIS were shown in Fig. 4A. As the concentration of ACE increased, the fluorescence signals of the T line weakened while those of the C line intensified, and the T/C became smaller, showing a typical competitive inhibition change pattern. Under optimal experimental conditions, the quantitative fitting curve for TRFLIS detection was shown in Fig. 4A. The standard curve equation was $Y = -0.80299X + 2.31502$. R^2 was 0.99248. According to $LOD = 3 \times SD \times 10^{(\frac{X-y}{z})}$ [31], the limit of detection (LOD) was 0.62 ng/mL. In addition, the same 20 blank samples were analyzed to establish the limit of quantification (LOQ) as $10 \times SD/S$. In the formula above, SD represented the standard deviation of the blank sample, while S represented the slope of the standard curve. The LOQ was 2.06 ng/mL. The linear range of the TRFLIS was 5–700 ng/mL. When the spiked concentration was 5 ng/mL, the fluorescence signal on the T line was significantly weaker than 0 ng/mL. So, the visual LOD of the TRFLIS was 5 ng/mL.

3.3.2. Stability and repeatability

To evaluate the stability and reproducibility of the test strips, the same batch of test strips were stored under dry conditions for 30 d, and the negative and positive samples with an ACE concentration of 25 ng/mL were tested on 1 d, 3 d, 6 d, 14 d, 20 d, and 30 d, followed by the analysis of the T/C ratio. Additionally, different batch of test strips were selected for inter-assay experiments to ensure the reproducibility of the results. The method's reproducibility was assessed by analyzing the intra-assay and inter-assay errors of T/C and T_0/C_0. The findings presented in Table 1 demonstrated high repeatability and stability of the method. The coefficients of variation (CV) for the intra-assay and inter-

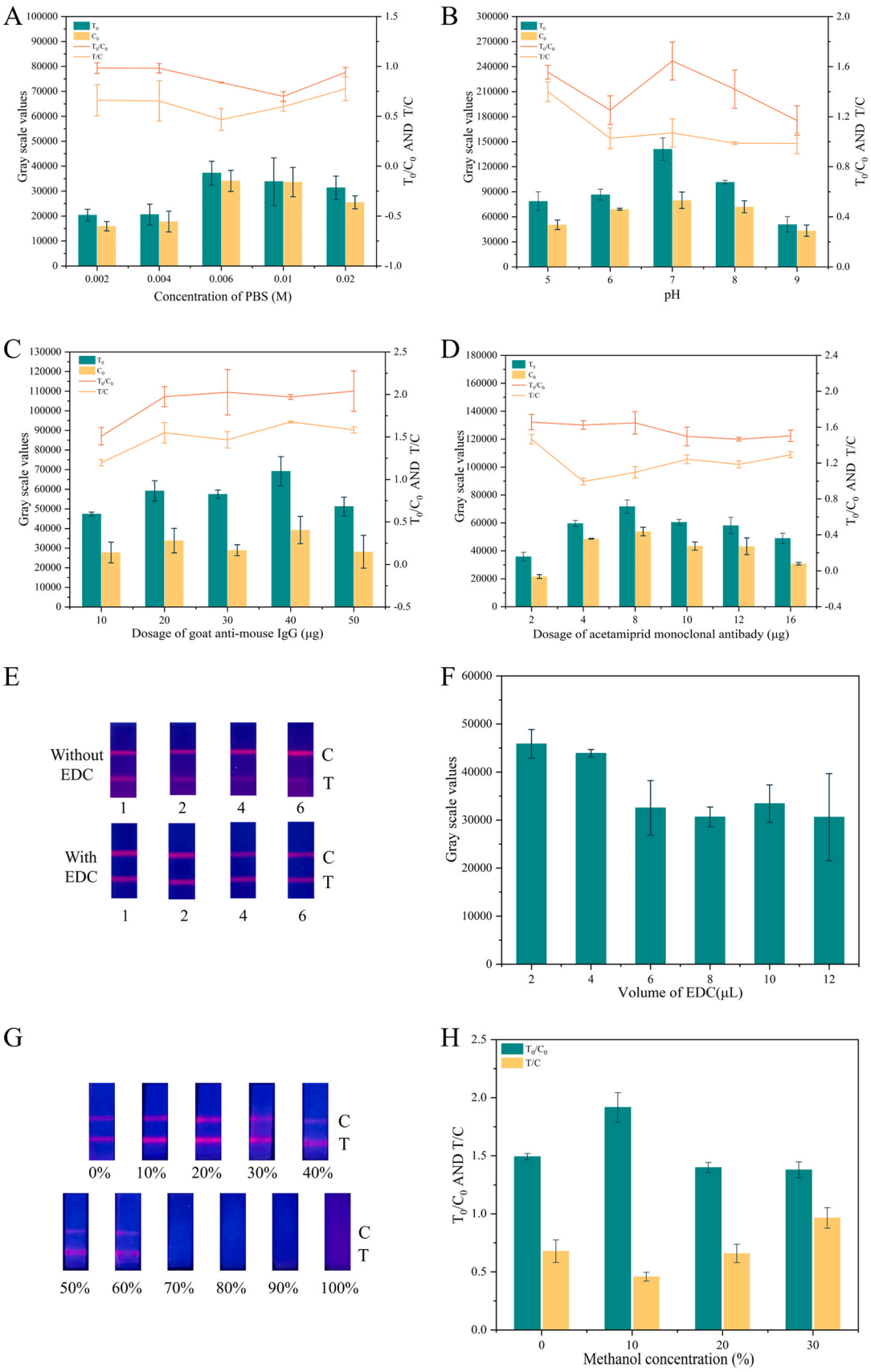

Fig. 3. Parameter optimization of TRFLIS (Column abscissa/parameter name): concentrations of PBS (A), pH (B), dosage of the GaMIgG (C), dosage of AAb (D); Comparison of fluorescence signals of TRFLIS with and without EDC (E); Test results of different volume EDC (F); Fluorescence signal of TRFLIS at 0 % to 100 % methanol dilution concentrations (G); Rate of change in different methanol dilution concentrations (H).

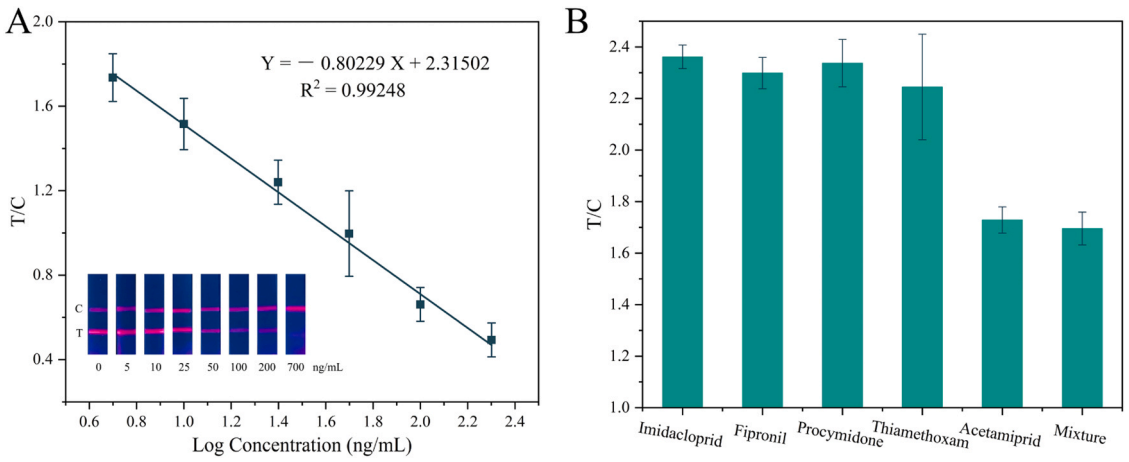

Fig. 4. Results from tests conducted with various concentrations of ACE standards and results observed when detected under a 365 nm UV lamp (A); Results of specificity experiments for TRFLIS (B).

Table 1
Stability experiment of TRFLIS (n = 3).

Intra-assay	T_0/C_0	T/C	Inter-assay	T_0/C_0	T/C
1	2.283779	1.743970	1	2.282546	1.745362
3	2.306400	1.700465	3	2.280735	1.725433
6	2.283777	1.743373	6	2.297683	1.785347
14	2.288973	1.764282	14	2.288767	1.723846
20	2.320400	1.725405	20	2.286493	1.763524
30	2.283779	1.743970	30	2.327584	1.742986
Mean	2.294518	1.736911	Mean	2.293968	1.747750
SD	1.31 %	1.84 %	SD	1.60 %	2.14 %
CV (%)	0.57 %	1.06 %	CV (%)	0.70 %	1.23 %

assay experiments were below 1.06 % and 1.23 %, respectively, indicating satisfactory stability and repeatability for the quantification of ACE using TRFLIS.

3.3.3. Specificity

To evaluate the specificity of the TRFLIS for detecting acetamiprid, a cross-reaction test was conducted against several structurally similar pesticides (thiamethoxam, fipronil, procymidone, imidacloprid) and ACE, each at a concentration of 25 ng/mL. The results were shown in Fig. 4B, the T/C of both ACE and the mixture were detected to change. The T/C of the other pesticides remained constant, indicating that ACE did not cross-reactive with these pesticides. Therefore, the TRFLIS had good specificity for the detection of acetamiprid.

3.4. Actual sample testing

Chinese cabbage, leek, and tomato were purchased from the market of Zibo city as representative vegetable samples. The ACE standard was added to three matrices to obtain the working curves of ACE in different vegetable matrices. The working curves and fluorescence signals of TRFLIS for tomato, leek, and Chinese cabbage matrices were visualized in Fig. 5A, B, and C, respectively. With tomato matrices, the TRFLIS showed a linear response range of 5–400 ng/mL, a LOD of 0.16 ng/mL and a LOQ of 0.53 ng/mL. And with leek matrices, the TRFLIS showed a linear response range of 5–300 ng/mL, a LOD of 0.60 ng/mL and a LOQ of 2.01 ng/mL. As the tomato and leek matrix were colored, it led to a narrower detection of TRFLIS. With Chinese cabbage matrices, the TRFLIS showed a linear response range of 5–700 ng/mL, a LOD of 0.41 ng/mL and a LOQ of 1.37 ng/mL. Since the color of the Chinese cabbage matrices was not affected by the pigment in Chinese cabbage, the Chinese cabbage matrices appeared colorless. Thus, the working curve under the Chinese cabbage matrix remained almost identical to 3.4.1 for the matrix-free sample solution. Additionally, the spiked recovery method was utilized to analyze three vegetable samples. The results depicted in Table 2 demonstrated spiked recovery from 98.90 % to 100.76 % for TRFIAS and 91.12 % to 103.06 % for LC-MS. In addition, the relative standard deviation (RSD) from 1.02 % to 2.97 % for TRFIAS and 1.74 % to 4.64 % for LC-MS. This analysis confirmed the high reliability of TRFIAS. Consequently, the findings suggested that TRFLIS held promising potential for acetamiprid detection.

3.5. Comparison of TRFLIS with other studies

Herein, the preparation of TRFLIS in this study was compared with other ACE detection methods. Table 3 summarized the information on acetamiprid detection. TRFLIS not only had a wider detection line but also had a lower LOD compared with colorimetry [39] and SERS [6] in detection ACE. In addition, In comparison to other analytical techniques, such as fluorescence [25,37], liquid chromatography-mass spectrometry (LC-MS) [13], aptamer strips [28,29] and aptamer lateral flow assay (ALFA) [27], although their LODs was lower than that of TRFLIS, TRFLIS exhibited superior capabilities in range of detection. Finally, when comparing TRFLIS with ECL [11,41] methods, both methods exhibit different advantages, yet TRFLIS exhibits superior performance in terms of detection time and convenience. TRFLIS offered expedited detection with simplified operational procedures, rendering it particularly suitable for scenarios necessitating swift results and user-friendly operation. The TRFLIS constructed in this study was able to maintain high fluorescence signals at lower marker concentrations, compared with the conventional AAb directly coupled to the TRFM [40]. The test strips prepared with the traditional method required about 7.5 μg of AAb per strip. In contrast, when GaMIgG was introduced as a sandwich protein, only 4 μg of AAb was required per strip. In addition, this strategy effectively reduced the LOD by 90 times compared with the traditional method. TRFLIS introduced GaMIgG as a sandwich protein to oriented AAb for better exposure of antigenic determinants. This strategy boosted sensitivity per unit antibody and led to cost savings.

4. Conclusion

In this study, a novel cross-linkable fluorescent probe with oriented antibody was constructed. Goat anti-mouse IgG (GaMIgG) was introduced as a sandwich protein for oriented modification of acetamiprid antibody (AAb), thereby exposing the antigenic determinants of AAb. This greatly reduced the used dosage of AAb and improved the sensitivity of time-resolved fluorescent lateral immunoassay strip (TRFLIS). In addition, the introduction of 1-ethyl-(3-dimethylaminopropyl)

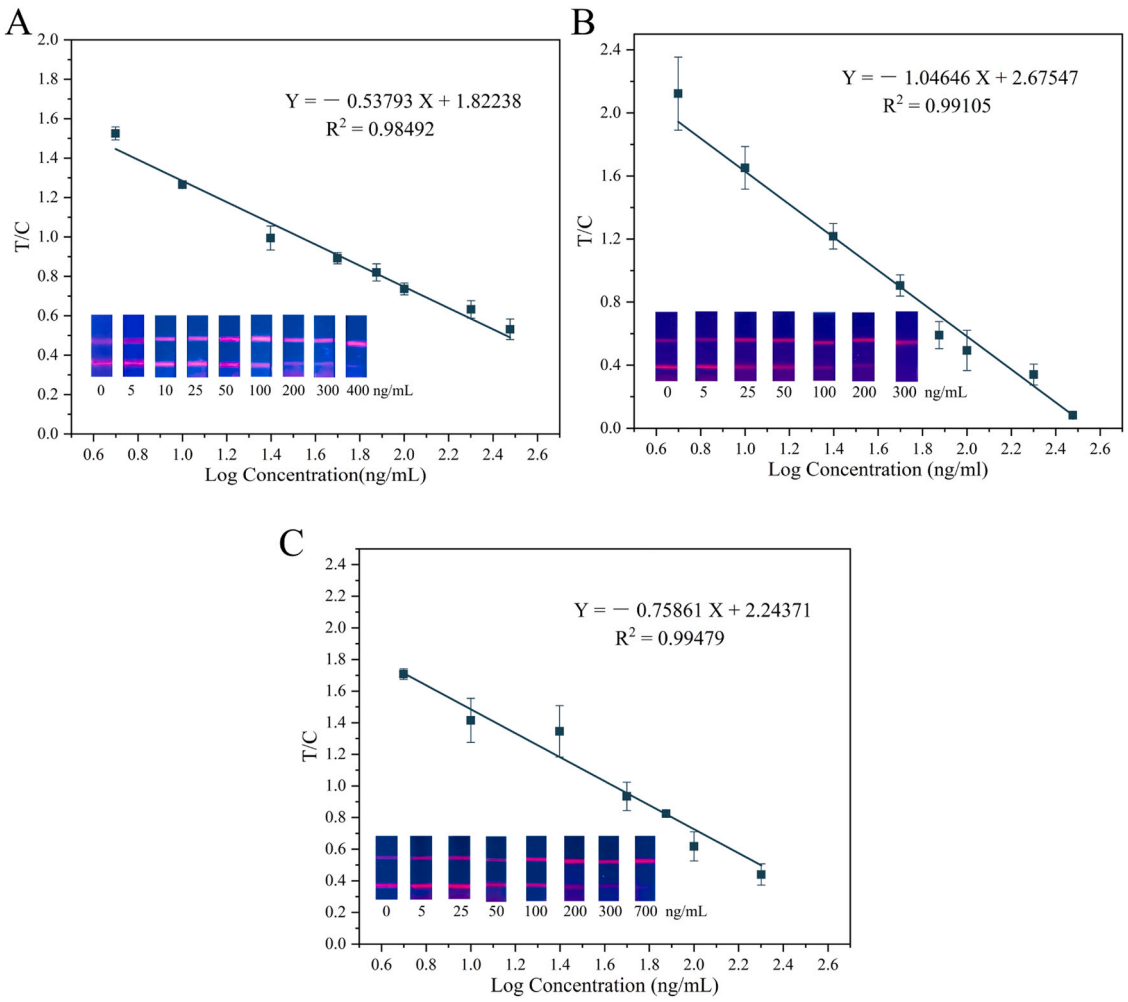

Fig. 5. Fitted curves under tomato matrices (A), leek matrices (B), and Chinese cabbage matrices (C).

Table 2
Recovery rates of different vegetables with addition experiment.

Sample type	Standard concentration (ng/mL)	TRFLIS (n = 3)			LC-MS (n = 3)		
		Mean (ng/mL)	Recovery (%)	RSD (%)	Mean (ng/mL)	Recovery (%)	RSD (%)
Cabbage	0	0.00	-	-	0.00	-	-
	50	50.23	100.46	2.92	47.07	94.15	3.12
	100	100.45	100.45	1.99	103.06	103.06	3.64
Leek	0	0.00	-	-	0.00	-	-
	50	49.50	99.00	1.02	45.56	91.12	4.64
	100	100.76	100.76	2.01	101.42	101.42	1.89
Tomato	0	0.00	-	-	0.00	-	-
	50	49.45	98.90	2.97	49.00	98.00	2.65
	100	100.37	100.37	1.93	101.53	101.53	1.74

carbodiimide hydrochloride as a cross-linking agent to form covalent bonds between GaMIgG and AAb improved the binding strength of the TRFM-GaMIgG-AAb, which improved the stability of TRFLIS. Under the optimal conditions, the T/C relationship with competitive inhibition of acetamiprid concentration was established in this study. The standard curve of the TRFLIS was constructed, and the R^2 was 0.99248. The limit of detection (LOD) of strip was as low as 0.62 ng/mL, the limit of quantification (LOQ) was 2.06 ng/mL and the visual LOD was 5 ng/mL. The TRFLIS was tested for practical applications using a variety of sample matrices, and it showed excellent detection accuracy, which validated their applicability in different samples. The TRFLIS exhibited strong performance in specificity, stability, repeatability, and sensitivity. It has many advantages such as cost-effectiveness, high sensitivity and specificity, simple and repaid operation, and short detection time. Especially in large-volume sample detection, it can rapidly exclude negative samples pre-screening, identify positive samples accurately and quickly for quantitative analysis, which significantly improves the detection efficiency. Therefore, this strip has a wide range of market application potential, especially suitable for meeting the needs of rapid daily testing.

CRediT authorship contribution statement

Peisen Li: Resources. **Shuxian Zhou:** Conceptualization. **Shengxi**

Table 3
Comparison with other ACE detection methods.

Method	LOD (ng/mL)	Detection range (ng/mL.)	Time (min)	References
LC-MS	0.60	3-314	60	[13]
Colorimetry	7.00	57-340	35	[39]
ALFA	0.17	1-150	20	[27]
Fluorescence	0.67	1-270	150	[25]
Fluorescence	0.08	5-220	30	[37]
ECL	0.09	11-6680	35	[41]
ECL	14.70	26-2557	35	[11]
Aptamer strip	0.33	5-200	15	[28]
Aptamer strip	0.17	1-150	15	[29]
SERS	2.66	5-60	15	[6]
TRFLIS	56.00	250-1750	15	[40]
TRFLIS	0.62	5-700	15	This study

Zhai: Funding acquisition. **Mingxin Zhao:** Supervision. **Xia Sun:** Writing – review & editing. **Yemin Guo:** Writing – review & editing. **Donghan Li:** Software, Formal analysis, Data curation, Conceptualization. **Haowei Dong:** Funding acquisition. **Zhengtao Li:** Investigation. **Haifang Wang:** Resources. **Jiashuai Sun:** Methodology. **Jingcheng Huang:** Validation.

Declaration of Competing Interest

The authors declare that they have no known competing financial interests or personal relationships that could have appeared to influence the work reported in this paper.

Data availability

The data that has been used is confidential.

Acknowledgements

This work was supported by the National Natural Science Foundation of China (No. 32372438, 31772068, 31872909), Funding Project for the Central Government to Guide the Development of Local Science and Technology (YDZX2022163), Shandong Province Major Applied Technology Innovation Project (SD2019NJ007), Technological Innovation Guidance Project of Department of Science &Technology of Gansu Province (22CX8NA023), Natural Science Foundation of Shandong Province (ZR202210150017) and Weifang Science and Technology Development Project (2021ZJ1103).

References

[1] Bax, D.V., Nair, M., Weiss, A.S., Farndale, R.W., Best, S.M., Cameron, R.E., 2021. Tailoring the biofunctionality of collagen biomaterials via tropoelastin incorporation and EDC-crosslinking. Acta Biomater 135, 150–163. https://doi.org/10.1016/j.actbio.2021.08.027.

[2] Chakraborty, T., Das, M., Lin, C.Y., Kao, C., 2023. Electrochemical detection of cystatin C by oriented antibody immobilization on streptococcal protein G-modified ZIF-8-$Cu_{1-x}Ni_x(OH)_2$@Cu core-shell nanostructured electrode. Mater Today Chem 27. https://doi.org/10.1016/j.mtchem.2022.101273.

[3] Dijk, T.C.V., Staalduinen, M.A.V., Sluijs, J.P.V.D., 2013. Macro-invertebrate decline in surface water polluted with imidacloprid. PLoS One 8 (5), e89837. https://doi.org/10.1371/journal.pone.0062374.

[4] Dong, H., Xu, D., Wang, G., Meng, X., Sun, X., Yang, Q., et al., 2022. Broad-specificity time-resolved fluorescent immunochromatographic strip for simultaneous detection of various organophosphorus pesticides based on indirect probe strategy. Anal Methods 14 (10), 1051–1059. https://doi.org/10.1039/D2AY00067A.

[5] Dong, H.W., An, X.S., Xiang, Y.D., Guan, F.K., Zhang, Q., Yang, Q.Q., et al., 2020. Novel time-resolved fluorescence immunochromatography paper-based sensor with signal amplification strategy for detection of deoxynivalenol. Sensors 20 (22). https://doi.org/10.3390/s20226577.

[6] Dong, S., He, K.L., Yang, J.H., Shi, Q.Y., Guan, L.J., Chen, Z.Y., et al., 2022. A simple mesoporous silica nanoparticle-based aptamers SERS sensor for the detection of acetamiprid. Spectrochim Acta Part a-Mol Biomol Spectrosc 283, 121725. https://doi.org/10.1016/j.saa.2022.121725.

[7] Fang, Q.K., Zu, Q., Hua, X.D., Lv, P., Lin, W.W., Zhou, D.H., et al., 2019. Quantitative determination of acetamiprid in pollen based on a sensitive enzyme-linked immunosorbent assay. Molecules 24 (7). https://doi.org/10.3390/molecules24071265.

[8] Gao, S.P., Niu, L.D., Zhou, R.Y., Wang, C., Zheng, X.Y., Zhang, D., et al., 2024. Significance of the antibody orientation for the lateral flow immunoassays: A mini-review. Int J Biol Macromol 257. https://doi.org/10.1016/j.ijbiomac.2023.128621.

[9] Ghanbari, M., Salavati-Niasari, M., Mohandes, F., 2021. Injectable hydrogels based on oxidized alginate-gelatin reinforced by carbon nitride quantum dots for tissue engineering. Int J Pharm 602. https://doi.org/10.1016/j.ijpharm.2021.120660.

[10] Ghanbari, M., Salavati-Niasari, M., Mohandes, F., Firouzi, Z., 2022. Modified silicon carbide NPs reinforced nanocomposite hydrogels based on alginate-gelatin by with high mechanical properties for tissue engineering. Arab J Chem 15 (1), 103520. https://doi.org/10.1016/j.arabjc.2021.103520.

[11] Guo, Y.M., Yang, F.Z., Yao, Y., Li, J.S., Cheng, S.T., Dong, H.W., et al., 2021. Novel Au-tetrahedral aptamer nanostructure for the electrochemiluminescence detection of acetamiprid. J Hazard Mater 401. https://doi.org/10.1016/j.jhazmat.2020.123794.

[12] Jayachandran, B., Parvin, T.N., Alam, M.M., Chanda, K., Balamurali, M.M., 2022. Insights on chemical crosslinking strategies for proteins. Molecules 27 (23) https://doi.org/10.3390/molecules27238124.

[13] Lee, H.S., Kim, S.W., El-Aty, A.M.A., Chung, H.S., Kabir, M.H., Rahman, M.M., et al., 2017. Liquid chromatography–tandem mass spectrometry quantification of acetamiprid and thiacloprid residues in butterbur grown under regulated conditions. J Chromatogr B 1055 172–177. https://doi.org/10.1016/j.jchromb.2017.04.021.

[14] Lee, J.E., Seo, J.H., Kim, C.S., Kwon, Y., Ha, J.H., Choi, S.S., et al., 2013. A comparative study on antibody immobilization strategies onto solid surface. Korean J Chem Eng 30, 1934–1938.

[15] Li, G., Wang, D., Zhou, A., Sun, Y., Zhang, Q., Poapolathep, A., et al., 2018. A rapid, onsite, ultrasensitive melamine quantitation method for protein beverages using time-resolved fluorescence detection paper. J Agric Food Chem 66 (22), 5671–5676. https://doi.org/10.1021/acs.jafc.8b01016.

[16] Li, G.H., Xu, L., Wu, W.Q., Wang, D., Jiang, J., Chen, X.M., et al., 2019. On-site ultrasensitive detection paper for multiclass chemical contaminants via universal bridge-antibody labeling: mycotoxin and illegal additives in milk as an example. Anal Chem 91 (3), 1968–1973. https://doi.org/10.1021/acs.analchem.8b04290.

[17] Li, G.Z., Guan, F.K., Zhao, S.C., Xu, H.H., Sun, J.S., Huang, J.C., et al., 2023. Immediate, sensitive and specific time-resolved fluorescent immunoassay strips based on immune competition for the detection of procymidone in vegetables. Food Control 147. https://doi.org/10.1016/j.foodcont.2022.109569.

[18] Li, G.Z., Sun, J.S., Li, J.H., Zhang, Y.L., Huang, J.C., Yue, F.L., et al., 2023. Paper-based biosensors relying on core biological immune scaffolds for the detection of procymidone in vegetables. Talanta 265. https://doi.org/10.1016/j.talanta.2023.124843.

[19] Li, M., Haiming, Sun, Jiadi, Ji, Jian, Ye, Yongli, Lu, Xin, Zhang, et al., 2021. Rapid, on-site, and sensitive detection of aflatoxin M1 in milk products by using time-resolved fluorescence microsphere test strip. Food Control 121, 107616 https://doi.org/10.1016/j.foodcont.2020.107616.

[20] Li, S.X., Liu, W.H., Liu, M.X., Chen, Y.Y., Zhang, F.Y., Wang, X.H., 2024. A sensitive lateral flow immunoassay relying on time-resolved fluorescent microspheres immune probe for determination of ceftiofur and its metabolite. Talanta 271. https://doi.org/10.1016/j.talanta.2023.125580.

[21] Li, Y.Y., Zhu, Z.W., Qu, W.L., Yang, Q., Liu, Y., Wang, Q., et al., 2023. A highly sensitive immunochromatographic assay for lead ions in drinking water based on antibody-oriented probe and silver enhancement. Eur Food Res Technol 249 (12), 3097–3103. https://doi.org/10.1007/s00217-023-04351-5.

[22] Li, Y.Y., Zhu, Z.W., Qu, W.L., Yang, Q., Liu, Y., Wang, Q., et al., 2023. Universal probe with oriented antibody to improve the immunochromatographic assay of lead ions in Procambarus clarkii. Food Qual Saf 7. https://doi.org/10.1093/fqsafe/fyad015.

[23] Liao, G., Jin, X., Chen, W., 2011. Application of high performance liquid chromatography in detection of imidacloprid and acetamiprid residuein tea. Guizhou Agric Sci 39 (4), 4.

[24] Lou, D., Fan, L., Cui, Y., Zhu, Y., Gu, N., Zhang, Y., 2018. Fluorescent nanoprobes with oriented modified antibodies to improve lateral flow immunoassay of cardiac troponin I. Anal Chem 90 (11), 6502–6508. https://doi.org/10.1021/acs.analchem.7b05410.

[25] Lu, X., Fan, Z.F., 2020. RecJf exonuclease-assisted fluorescent self-assembly aptasensor for supersensitive detection of pesticides in food. J Lumin 226. https://doi.org/10.1016/j.jlumin.2020.117469.

[26] Majdinasab, M., Zareian, M., Zhang, Q., Li, P., 2019. Development of a new format of competitive immunochromatographic assay using secondary antibody-europium nanoparticle conjugates for ultrasensitive and quantitative determination of ochratoxin A. Food Chem 275, 721–729. https://doi.org/10.1016/j.foodchem.2018.09.112.

[27] Mao, M., Sun, F., Wang, J., Li, X., Pan, Q., Peng, C., et al., 2023. Delayed delivery of chromogenic substrate to nanozyme amplified aptamer lateral flow assay for acetamiprid. Sens Actuators B: Chem 385, 133720. https://doi.org/10.1016/j.snb.2023.133720.

[28] Mao, M.X., Chen, X.J., Cai, Y.N., Yang, H.J., Zhang, C.Z., Zhang, Y., et al., 2023. Accelerated and signal amplified nanozyme-based lateral flow assay of acetamiprid based on bivalent triple helix aptamer. Sens Actuators B: Chem 378. https://doi.org/10.1016/j.snb.2022.133148.

[29] Mao, M.X., Sun, F.X., Wang, J., Li, X.P., Pan, Q.L., Peng, C.F., et al., 2023. Delayed delivery of chromogenic substrate to nanozyme amplified aptamer lateral flow assay for acetamiprid. Sens Actuators B: Chem 385. https://doi.org/10.1016/j.snb.2023.133720.
[30] Mao, X.Y., Yu, B.E., Li, Z.J., Li, Z.P., Shi, G.Q., 2022. Comparison of lateral flow immunoassays based on oriented and nonoriented immobilization of antibodies for the detection of aflatoxin B1. Anal Chim Acta 1221. https://doi.org/10.1016/j.aca.2022.340135.
[31] Majdinasab, Marjan, Sheikh-Zeinoddin, Mahmoud, Soleimanian-Zad, Sabihe, Li, Peiwu, Zhang, Qi, 2015. A reliable and sensitive time-resolved fluorescent immunochromatographic assay (TRFICA) for ochratoxin A in agro-products. Food Control 47, 126–134. https://doi.org/10.1016/j.foodcont.2014.06.044.
[32] Nair, M., Johal, R.K., Hamaia, S.W., Best, S.M., Cameron, R.E., 2020. Tunable bioactivity and mechanics of collagen-based tissue engineering constructs: A comparison of EDC-NHS, genipin and TG_2 crosslinkers. Biomaterials 254. https://doi.org/10.1016/j.biomaterials.2020.120109.
[33] Niazi, S., Khan, I.M., Yu, Y., Pasha, I., Wang, Z., 2019. A "turnon" aptasensor for simultaneous and time-resolved fluorometric determination of zearalenone, trichothecenes A and aflatoxin B1 using WS_2 as a quencher. Microchim Acta 186 (8), 1–10. https://doi.org/10.1007/s00604-019-3570-y.
[34] EFSA Panel on Plant Protection Products and their Residues (PPR, 2013. Scientific opinion on the developmental neurotoxicity potential of acetamiprid and imidacloprid. EFSA J 11 (12), 3471. https://doi.org/10.2903/j.efsa.2013.3471.
[35] Sun, J.D., Li, M., Xing, F.G., Wang, H.M., Zhang, Y.Z., Sun, X.L., 2022. Novel dual immunochromatographic test strip based on double antibodies and biotin-streptavidin system for simultaneous sensitive detection of aflatoxin M1 and ochratoxin a in milk. Food Chem 375. https://doi.org/10.1016/j.foodchem.2021.131682.
[36] Sun, J.S., Liu, W.Z., He, Z.Y., Li, B.X., Dong, H.W., Liu, M.Y., et al., 2024. Novel electrochemiluminescence aptasensor based on AuNPs-ABEI encapsulated TiO_2 nanorod for the detection of acetamiprid residues in vegetables. Talanta 269. https://doi.org/10.1016/j.talanta.2023.125471.
[37] Wang, J.L., Wu, Y.G., Zhou, P., Yang, W.P., Tao, H., Qiu, S.Y., et al., 2018. A novel fluorescent aptasensor for ultrasensitive and selective detection of acetamiprid pesticide based on the inner filter effect between gold nanoparticles and carbon dots. Analyst 143 (21), 5151–5160. https://doi.org/10.1039/c8an01166d.
[38] Wu, Q., Yao, L., Qin, P., Xu, J., Sun, X., Yao, B., et al., 2021. Time-resolved fluorescent lateral flow strip for easy and rapid quality control of edible oil. Food Chem 357, 129739. https://doi.org/10.1016/j.foodchem.2021.129739.
[39] Xu, C., Lin, M., Song, C., Chen, D., Bian, C., 2022. A gold nanoparticle-based visual aptasensor for rapid detection of acetamiprid residues in agricultural products using a smartphone. RSC Adv 12 (9), 5540–5545. https://doi.org/10.1039/d2ra00348a.
[40] Xu, R., Xiang, Y.D., Shen, Z., Li, G.Z., Sun, J.S., Lin, P.Y., et al., 2023. Portable multichannel detection instrument based on time-resolved fluorescence immunochromatographic test strip for on-site detecting pesticide residues in vegetables. Anal Chim Acta 1280, 9. https://doi.org/10.1016/j.aca.2023.341842.
[41] Xu, Y.W., Zhang, W., Shi, J.Y., Li, Z.H., Huang, X.W., Zou, X.B., et al., 2020. Impedimetric aptasensor based on highly porous gold for sensitive detection of acetamiprid in fruits and vegetables. Food Chem 322. https://doi.org/10.1016/j.foodchem.2020.126762.
[42] Yao, X., Wang, Z., Dou, L., Zhao, B., He, Y., Wang, J., et al., 2019. An innovative immunochromatography assay for highly sensitive detection of 17β-estradiol based on an indirect probe strategy. Sens Actuators B: Chem 289, 48–55. https://doi.org/10.1016/j.snb.2019.03.078.
[43] Zha, C.A.Y., An, X.S., Zhang, J.L., Lin, W., Zhang, Q., Yang, Q.Q., et al., 2022. Indirect signal amplification strategy with a universal probe-based lateral flow immunoassay for the rapid quantitative detection of fumonisin B1. Anal Methods 14 (7), 708–716 https://doi.org/10.1039/d1ay01625c.
[44] Zhang, B., Pan, X., Venne, L., Dunnum, S., Mcmurry, S.T., Cobb, G.P., et al., 2008. Development of a method for the determination of 9 currently used cotton pesticides by gas chromatography with electron capture detection. Talanta 75 (4), 1055–1060. https://doi.org/10.1016/j.talanta.2008.01.032.